

## COULOMB EXCITATION OF SEPARATED TIN ISOTOPES

D. G. ALKHAZOV, D. S. ANDREEV, K. I. EROKHINA, and I. Kh. LEMBERG

Leningrad Physico-Technical Institute, Academy of Sciences, U.S.S.R.

Submitted to JETP editor June 3, 1957; resubmitted October 5, 1957

J. Exptl. Theoret. Phys. (U.S.S.R.) 33, 1347-1358 (December, 1957)

Alpha particles accelerated to 14.5 Mev in a cyclotron were used to investigate the Coulomb excitation of nuclear levels of separated tin isotopes. A number of previously unknown states were excited, for which we measured the energy and the reduced probability of transition from the ground state. The lifetimes of the first excited states of even-even tin isotopes were calculated. The lifetimes lie in the range from  $5 \times 10^{-13}$  sec ( $\text{Sn}^{114}$ ) to  $16 \times 10^{-13}$  sec ( $\text{Sn}^{124}$ ).

## 1. INTRODUCTION

THE study of Coulomb excitation of rotational levels of nuclei in the mass region  $A = 150 - 190$  has played an important part in checking and improving the concepts of the uniform model. At the present stage of development of the uniform model, it is of interest to study Coulomb excitation of levels in nuclei which are outside the rotational region. It is especially important to excite levels of even-even nuclei, where the internal structure does not affect the angular momentum of the nucleus. However, efforts to excite levels by Coulomb interaction have certainly not been successful for all nuclei outside the rotational region. Thus, attempts<sup>1,2</sup> at Coulomb excitation of levels in tin, using  $\alpha$  particles with an energy  $E_\alpha$  up to 7 Mev, gave no results.

The cross section for Coulomb excitation via electric quadrupole transition is given by the formula

$$\sigma = 2\mu (E - \Delta E) B(E2) f_2(\xi) / Z_2^2 \hbar^2 e^2, \quad (1)$$

where

$$\xi = \frac{Z_1 Z_2 e^2 V_\mu}{\hbar V^2} \left( \frac{1}{V E - \Delta E} - \frac{1}{V E} \right) \approx \frac{Z_1 Z_2 e^2 \mu^{1/2}}{\hbar V^2} \frac{\Delta E}{2E^{3/2}}, \quad (2)$$

$\mu$  is the reduced mass of the bombarding particle,  $Z_1$  the number of protons in its nucleus,  $E$  and  $(E - \Delta E)$  are the energy of the nucleus before and after collision,  $Z_2$  is the number of protons in the nucleus of the target atom,  $B(E2)$  is the reduced probability for electric quadrupole transition of the nucleus from its ground state to the particular excited state,  $\Delta E$  is the nuclear excitation energy, and  $f_2(\xi)$  is the Coulomb excitation function, which for not too low values of  $\xi$  drops almost exponentially with increasing  $\xi$ . A graph of  $f_2(\xi)$  is given in Ref. 3.

Considering that the values of  $\Delta E$  for the low-lying levels of tin are large, and that the values of  $B(E2)$  for excitation of vibrational or single-particle levels are small compared to the values for excitation of rotational states, it follows from formulas (1) and (2) that the cross section for excitation of levels in tin should be very small if  $\alpha$  particles with  $E_\alpha$  below 7 Mev are used. However, as our computations show, when  $E_\alpha$  is increased from 7 to 13 Mev the thick target yield (with  $\Delta E = 1.2$  Mev) increases by a factor of 200.

To excite nuclear levels in tin, we used  $\alpha$  particles accelerated to 14.5 Mev in a cyclotron. Previously most experiments on Coulomb excitation have been done with particles accelerated in an electrostatic generator. Then the energy spread in the beam is very small and it is also easy to change the beam energy. However, raising the energy of particles accelerated in an electrostatic generator presents well-known difficulties so that up to now, in work on Coulomb excitation, particles with energies not exceeding 7 Mev have been used.

The energy spread of the particles in the extracted cyclotron beam does not exceed  $\pm 2\%$ . Our computations show that if, instead of a monochromatic beam with  $E_\alpha = 10$  Mev, a beam with a Gaussian energy distribution with 2% half-width is used for Coulomb excitation, the error in the determination of  $B(E2)$

does not exceed 1%. If, as an extreme case, we assume that the energies of all the particles in the beam differ from the nominal energy by 2%, the resultant error in the determination of  $B(E_2)$  is 15% for  $E_\alpha = 10$  Mev and 10% for  $E_\alpha = 14.5$  Mev, if  $\Delta E = 1.2$  Mev. Since the overall error in the determination of  $B(E_2)$  in Coulomb excitation experiments, due to uncertainties in various other factors, is usually not less than 20%, the resultant error if we include the possible error associated with the energy spread is  $\sqrt{20^2 + 15^2}$ , i.e., 25%.

Increasing the value of  $E_\alpha$  by a factor of 2 compared to the values used in other work on Coulomb excitation should lead to a large increase in the background of radiations which are emitted in reactions which occur via the formation of a compound nucleus. Preliminary estimates showed that, for  $E \approx (0.6 - 0.8) E_B$ , the cross section for compound nucleus formation is less than or comparable with the cross section for Coulomb excitation for nuclei in the middle of the periodic table. In studying Coulomb excitation, the most important contamination comes from inelastic scattering ( $\alpha, \alpha'$ ) which occurs via compound nucleus formation, since  $\gamma$  rays of the same energy are then emitted as in the ( $\alpha, \alpha'$ ) process which occurs via Coulomb excitation. However, the relative probability for decay of the compound nucleus via the ( $\alpha, \alpha'$ ) channel is much less than the probability for decay into ( $\alpha, n$ ), ( $\alpha, p$ ), and ( $\alpha, \alpha$ ) channels.

We should mention that the theoretical energy dependence of the cross section for Coulomb excitation has been verified in many experiments over a wide range of energies of the bombarding particles. Consequently, experimental determination of the excitation function enables us to decide whether a particular line is the result of Coulomb excitation or of compound nucleus formation.

We should mention that the theoretical energy dependence of the cross section for Coulomb excitation has been verified in many experiments over a wide range of energies of the bombarding particles. Consequently, experimental determination of the excitation function enables us to decide whether a particular line is the result of Coulomb excitation or of compound nucleus formation.

## 2. EXPERIMENTAL METHOD

A beam of  $\alpha$  particles with energies up to 14.5 Mev was obtained at the cyclotron of the Physico-Technical Institute of the Academy of Sciences. Using a standard deflector, the beam of  $\alpha$  particles was brought out into

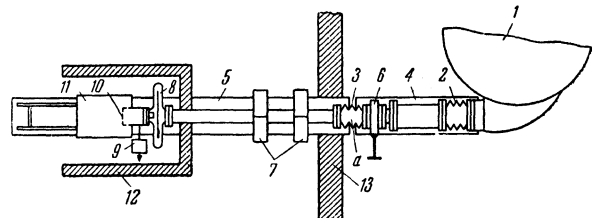


**FIG. 1.** Arrangement of apparatus (top view): 1 — cyclotron chamber; 2 and 3 — sylphon bellows; 4 and 5 — beams, linked by a universal joint which makes possible rotation of beam 5 around point a in any direction and thus simplifies setting the system so that the particle beam strikes the center of the target; 6 — vacuum gate, which is closed for changing targets; 7 — magnetic lenses; 8 — glass section for observing scintillation screen to enable focusing the beam; 9 — current integrator input stage; 10 — target; 11 — FEU-S photomultiplier in iron shield; 12 — lead shield against  $\gamma$  radiation from cyclotron; 13 — shield against neutrons from cyclotron. It consists of paraffin blocks for moderating the neutrons and cadmium sheets to absorb them.

an evacuated aluminum tube. A series of lead diaphragms were arranged inside the tube to prevent the particles from striking the tube walls. The beam was focused on the target by a system of two magnetic quadrupole lenses.\* The target was placed on the bottom of an insulated metallic cup which served as a Faraday cup. The amount of charge carried by the  $\alpha$  particles bombarding the target was measured using an electronic integrator, which was calibrated before and after each experiment. To eliminate errors in beam current measurement due to secondary electron emission, a ring was placed in front of the Faraday cup and was kept at 90 volts negative with respect to it. The  $\gamma$  radiation emitted in de-excitation of the excited levels was detected with a scintillation spectrometer. The FEU-S photomultiplier, the NaI (Tl) crystal (diameter 29 mm and  $l_k = 14$  mm), and a cathode follower were kept inside an effective magnetic shield consisting of three concentric iron cylinders. To avoid errors resulting from the anisotropy in the angular distribution of the  $\gamma$  quanta emitted after Coulomb excitation, it is desirable to achieve an arrangement of the apparatus corresponding to a solid angle  $\sim 2\pi$ . In our experiments the front surface of the crystal was at a distance of 4.35 mm from the target. Under conditions of near geometry, small displacements of the crystal relative to the target give a sizeable change of solid angle, i.e., of counting efficiency. We therefore took special measures to assure a unique geometry: the photomultiplier and crystal were pressed against the bottom of the Faraday cup by means of a spring, the bottom of

\*The parameters of the magnetic lenses and some additional information concerning procedure are given in other papers.<sup>4,5</sup>

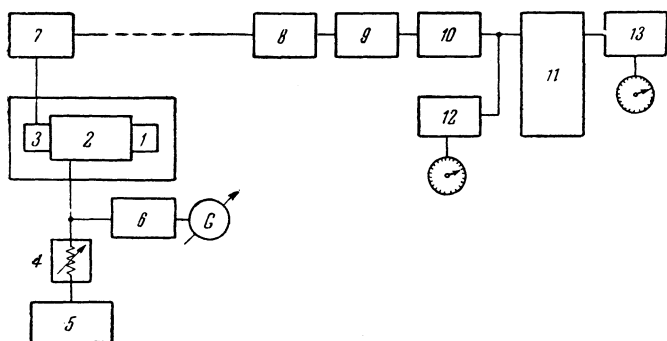


FIG. 2. Block diagram of the  $\gamma$ -spectrometer:

1 — scintillator; 2 — photomultiplier; 3 — cathode follower; 4 — regulating resistor for maintaining constant voltage on the photomultiplier; 5 — dry battery; 6 — potentiometer circuit for voltage measurement; 7 — heavy-duty cathode follower, feeding into a 50 meter line; 8 — linear amplifier; 9 — pulse stretcher; 10 — window amplifier; 11 — 50-channel pulse-amplitude analyzer; 12 — scaling circuit for  $N_0$  counts; 13 — scaling circuit for  $N_B$  counts.

compared the yield of  $\gamma$  radiation emitted after Coulomb excitation of tantalum when the target was a tantalum disc 8.2 mm in diameter placed at the center, and when the tantalum disc had a diameter equal to the inner diameter of the aluminum cup. In experiments on Coulomb excitation of tellurium, a water suspension of metallic tellurium powder was deposited in droplets on the central portion of the backing. After evaporation of the water, the tellurium powder was pressed in the same way as for the tin samples. In all cases, the target thickness was sufficient to slow down the  $\alpha$  particles to an energy at which the Coulomb excitation yield was insignificant. At first we had intended, in getting the Coulomb excitation function, to vary the  $\alpha$ -particle energy by placing aluminum foils of various thicknesses along the beam path. However, it turned out that even when the foils were located 60 cm from the target, the background rose as a result of  $\alpha$ -particle reactions in Al by an order of magnitude compared with its level when the foils were absent. It was not possible to reduce the background by moving the foils further from the target, since the intensity of the  $\alpha$ -particle beam incident on the target was diminished because of Rutherford scattering. For this same reason (increase in Rutherford scattering with increasing  $Z_2$ ), we could not reduce the background from nuclear reactions by replacing the aluminum by an element with higher atomic number. We succeeded in using the foils only when the yield from Coulomb excitation was large compared to the background (for example, in experiments on Coulomb excitation of Ta and Ag which were done to calibrate the apparatus). We therefore avoided the use of the foils in getting the Coulomb excitation function, and changed the  $\alpha$ -particle energy in steps, by readjusting the cyclotron. Altogether, we used four fixed values of the  $\alpha$ -particle energy: 10.15, 11.45, 13.1, and 14.5 Mev.

A block diagram of the  $\gamma$ -spectrometer is shown in Fig. 2. A blocking arrangement was provided in the circuit of the 50-channel analyzer, to cut off the analyzer input from the window-amplifier output for a period of  $10\mu$  sec after the acceptance of a pulse by the analyzer. The window-amplifier circuit is linear, and sends pulses to the analyzer input having amplitudes in the range from  $V_1$  to  $V_2$ . The values for the lower and upper limits of the window-amplifier output could be varied in the range from 5 to 80 volts. The purpose of the window amplifier is to reduce the overall load on the analyzer. To calculate the absolute values of the cross section, the number of counts in the channels must be multiplied by the ratio  $N_0/N_B$ , where  $N_0$  is the total number of pulses passed by the window amplifier, and  $N_B$  is the number of pulses accepted for analysis by the amplitude analyzer.

The energy calibration of the  $\gamma$ -spectrometer was done using  $\gamma$  rays from  $\text{Hg}^{203}$  (279.5 kev);  $\text{Cs}^{137}$  (661 kev), and  $\text{Zn}^{65}$  (1120 kev).

the copper Faraday cup was made thick enough so that it would not bend under atmospheric pressure; finally, a special arrangement assured good contact between the target backing and the bottom of the Faraday cup.

Between the target and the front surface there were the following layers of material, which partially absorbed the  $\gamma$  rays from the target:  $400\mu$  Cu, 1.3 mm Al,  $100\mu$  mica, 1 mm  $\text{MgO}$ ,  $50\mu$  Pb, and 1.5 mm air.

A diagram of the apparatus is shown in Fig. 1. The targets were separated isotopes of tin in the form of metallic samples. The target backing was a  $50\mu$  thick layer of lead pressed into an aluminum cap 1 mm high, 28 mm in diameter, with a base  $300\mu$  in thickness. The metallic tin sample was placed at the center of the target and was pressed onto the backing along with a lead disc which was placed on top of it and which had an opening at its center 8.2 mm in diameter. The fraction of the flux striking the tin target was determined in separate experiments in which we

## 3. HANDLING OF RESULTS

The theoretical value of the total yield  $Y$ , per bombarding particle, for excitation of a state with energy  $\Delta E$  in bombardment of a thick target, is

$$Y = \int \sigma N_1 dx = \frac{2\mu N_A}{A_2 Z_2^2 \hbar^2} \frac{B(E_2)}{e^2} \int_{\Delta E}^{E_{\max}} \frac{(E - \Delta E) f_2(\xi) dE}{dE/d\rho x}. \quad (3)$$

$N_1$  is the number of nuclei of the isotope per cc,  $N_A$  is Avogadro's number,  $A_2$  is the mass number of the isotope,  $dE/d\rho x$  is the stopping power of the target material;  $E_{\max}$  is the collision energy corresponding to the initial energy of the  $\alpha$  particles bombarding the target.

In the experiment the yield is found by taking the spectrum of Coulomb excitation and determining the number of  $\gamma$  quanta per microcoulomb,  $S_{ph}$ , recorded under the full energy peak. The full energy peak corresponds to complete absorption of the energy of the  $\gamma$  quantum in the crystal, and

$$Y = 3.2 \cdot 10^{-13} S_{ph} (1 + \alpha_t) / \eta \epsilon_{ph} \omega A_\gamma. \quad (4)$$

In formula (4),  $\alpha_t$  is the total internal conversion coefficient [the factor  $(1 + \alpha_t)$  takes account of the possibility of de-excitation via conversion],  $\epsilon_{ph}$  is the fraction of  $\gamma$  quanta recorded under the full energy peak, relative to the total number of  $\gamma$  quanta striking the crystal;  $\omega$  is the solid angle in units of  $4\pi$ ;  $A_\gamma$  is a factor which takes account of the absorption of the  $\gamma$  rays in the target and in the materials which are located between the target and the crystal;  $\eta$  is the percentage content of the particular isotope in the target. The value of  $dE/d\rho x$  was calculated from the formula

$$-dE/d\rho x = (4\pi e^4 Z_1^2 Z_2^2 N_A / m v^2 A_2) L, \quad (5)$$

where  $m$  is the electron mass and  $v$  the velocity of the incident particle. To compute  $L$ , we used the semi-empirical formula:<sup>6</sup>

$$L = 1.55 v \hbar / e^2 Z_2^{1/2}. \quad (6)$$

Thus,

$$-dE/d\rho x = 4.38 \pi e^2 \hbar N_A Z_1^2 Z_2^{1/2} \mu^{1/2} / m A_2 E^{1/2} = K E^{-1/2}. \quad (7)$$

To check whether formula (7) could be used reliably for determining  $dE/d\rho x$ , we used the formula for Cu, Sn, Pb, for four values of  $E_\alpha$  in the range from 15 to 10 Mev, and compared the results with data of Rybakov<sup>7</sup> and Segre.<sup>8</sup> The agreement was good. The difference did not exceed 5% for Cu and Sn, and was less than 10% for Pb.

The final expression for determining  $B(E_2)$  when  $\alpha$  particles are used for Coulomb excitation is gotten from formulas (3) – (6) and has the form

$$\frac{B(E_2)}{e^2} = 6.254 \cdot 10^{-10} \frac{Z_2^{1/2}}{\mu^{1/2} \eta} \left\{ S_{ph} (1 + \alpha_t) / \epsilon_{ph} \omega A_\gamma \int_{\Delta E}^{E_{\max}} (E - \Delta E) E^{1/2} f_2(\xi) dE \right\}, \quad (8)$$

where  $E$  and  $\Delta E$  are in Mev,  $\mu$  is in mass units and  $B(E_2)/e^2$  in units of  $10^{-48} \text{ cm}^4$ . The values of the integral were computed by graphical integration.

The internal conversion coefficients are very small (less than 1%) for the high-energy levels excited in tin, and  $\alpha_t$  was set equal to zero in the computations.

The estimate of the overall efficiency  $\epsilon_{ph} \omega A_\gamma$  of the scintillation spectrometer was done as follows: the values of  $\epsilon_{ph}$ ,  $\omega$ , and  $A_\gamma$  were calculated individually as a function of the  $\gamma$ -ray energy  $E_\gamma$ , and a graph was made of the product of these quantities as a function of  $E_\gamma$  in the range of  $E_\gamma$  from 0 to 1.4 Mev.  $\epsilon_{ph}$  was determined from the relation

$$\epsilon_{ph} = (1 - \exp \{-\mu_t l\}) p^*, \quad (9)$$

where  $\mu_t$  is the total absorption coefficient for the  $\gamma$  rays in the material of the crystal,  $l$  is the height of the crystal, and  $p^*$  is the fraction of the  $\gamma$  quanta recorded under the full energy peak relative to the total number recorded over the whole spectrum. The magnitude of  $p^*$  depends on the energy of  $\gamma$  quanta, the dimensions of the crystal and the geometry for recording the  $\gamma$  radiation (the shape of the source, its

position and distance from the crystal). To calculate  $\epsilon_{ph}$ , we used the values of  $\mu_t$  and  $p^*$  given in Ref. 9. The solid angle was computed from the formula

$$\omega = \frac{1}{2} \left( 1 - \frac{1}{\sqrt{1 + r^2/h'^2}} \right), \quad (10)$$

where  $r$  is the radius of the crystal,  $h' = h + l'$ ,  $h$  is the distance from the target to the front face of the crystal,  $l'$  is the distance to the plane in the crystal such that equal numbers of  $\gamma$  rays are absorbed on each side of it, i.e.,

$$1 - \exp\{-\mu_t l'\} = \frac{1}{2} (1 - \exp\{-\mu_t l\}); \quad (11)$$

$$l' = -\frac{1}{\mu_t} \ln \frac{1}{2} (1 + \exp\{-\mu_t l\}). \quad (12)$$

Values of  $\gamma$ -ray absorption coefficients used in calculating  $A_\gamma$  were taken from Ref. 10.

To check the computations, we determined the counting efficiency at the full energy peak for  $\gamma$  quanta with  $E_\gamma = 1.33$  Mev ( $\text{Co}^{60}$ ) and 0.661 Mev ( $\text{Cs}^{137}$ ). For this purpose we prepared thin sources of  $\text{Co}^{60}$  and  $\text{Cs}^{137}$ , having the same shape as the targets used in the experiments on Coulomb excitation. The in-

tensity of these sources was determined using a  $4\pi$ -geometry  $\beta$ -counter.<sup>†</sup> The gamma spectra of  $\text{Co}^{60}$  and  $\text{Cs}^{137}$  were taken in the same apparatus, keeping the same geometry and with the same absorbing materials present as in the experiments on Coulomb excitation. The values of total efficiency found by experiment exceeded the calculated values by a factor of 1.30 for  $E_\gamma = 661$  keV and a factor of 1.27 for  $E_\gamma = 1.33$  Mev. In computing values of  $B(E2)$  from the Coulomb excitation experiments, we used our computed values of the total efficiency multiplied by 1.28.

The difference between the computed and measured values of the overall efficiency is apparently explained by the fact that our experiments were carried out under conditions of "near geometry," whereas the values of  $\mu_t$  and  $p^*$  are given<sup>9</sup> for the case where the beam of  $\gamma$  rays is incident parallel to the axis of the crystal, i.e., for "far geometry." The problem of the dependence of the efficiency of recording  $\gamma$  rays on the distance of the source from the crystal is investigated in Ref. 12. Using the data of this paper, we recomputed the values of the overall efficiency for the case of near geometry. The computed values corrected in this fashion were in good agreement with the data obtained experimentally.

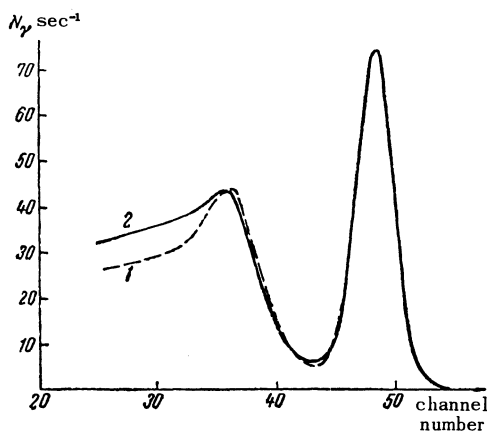


FIG. 3. 1 — theoretical line shape for  $E_\gamma = 1.12$  Mev, computed from data of Ref. 9 using the measured values for the energy resolution of the spectrometer; 2 — experimental spectrum of  $\text{Zn}^{65}$   $\gamma$  radiation ( $E_\gamma = 1.12$  Mev).

The magnitude of  $S_{ph}$  was determined from the area under the full energy peak. The area of the peak, the position of the maximum, the height of the maximum and the peak width all depend on how one draws the background curve. To determine the value of  $S_{ph}$  more accurately, we used the theoretical line shape constructed from data given in Ref. 9. By repeated trials with slight changes in the position of the maximum, its height and the half width of the peak, we tried to subtract the theoretical spectrum from the observed spectrum and obtain a smooth background curve which joined continuously to the experimentally observed spectrum of the background to the right of the peak. To check the computations of the theoretical line shape, the shape of the 1.12 Mev line from  $\text{Zn}^{65}$  was measured with the scintillation spectrometer. The results are shown in Fig. 3. The figure shows that the experimental and computed spectra are in good agreement. The somewhat higher intensity of the experimental spectrum in the low-energy region is explained by the contribution from  $\gamma$  quanta scattered in the iron cylinders which surrounded the photomultiplier and crystal.

In determining  $S_{ph}$  we also had to take account of the presence of other isotopes in the sample. Using the known values for the content of isotopic impurities, the energies of levels excited in them, and the values of  $B(E2)$  for excitation of these levels, we could calculate the theoretical spectrum for the lines

<sup>†</sup> The counter was prepared on the basis of data presented in Ref. 11.

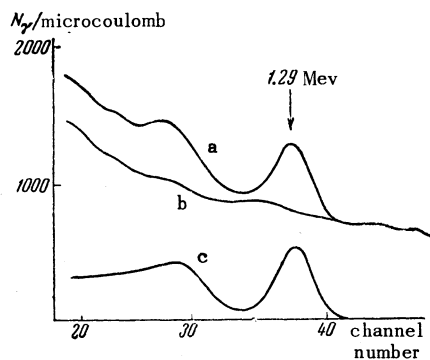


FIG. 4

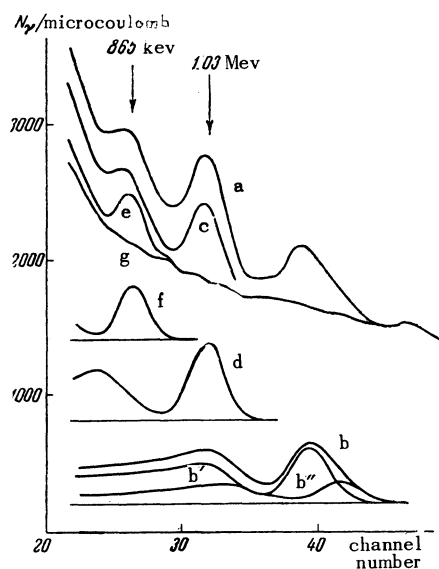


FIG. 5

FIG. 4. Gamma spectrum emitted after bombardment of  $\text{Sn}^{116}$  with 13.1 Mev  $\alpha$  particles: a — experimental spectrum; b — theoretical line shape for  $\gamma$  quanta with  $E_\gamma = 1.29$  Mev; c — background curve after subtracting theoretical line shape from experimental spectrum.

FIG. 5. Gamma spectrum emitted after bombardment of  $\text{Sn}^{117}$  with 13.1 Mev  $\alpha$  particles: a — experimental spectrum; b' and b'' — theoretical line shapes for  $E_\gamma = 1.24$  and 1.31 Mev; b — curve obtained by adding ordinates of curves b' and b''; c — spectrum after subtracting curve b; d — theoretical line shape for  $E_\gamma = 1.03$  Mev. e — spectrum after subtracting curve d; f — theoretical shape for  $E_\gamma = 865$  keV; g — background curve.

emitted in the de-excitation of the states excited in the impurity isotope. This spectrum was subtracted from the spectrum measured in the experiment.

Figures 4 and 5 show  $\gamma$  spectra emitted after Coulomb excitation of  $\text{Sn}^{116}$  and  $\text{Sn}^{117}$ .

In calculating values of  $B(E2)$  for lines excited in even-even isotopes, the anisotropy of the angular distribution of the  $\gamma$  rays emitted after Coulomb excitation was taken into account. The values of  $B(E2)$  obtained from formula (8) omitting the effects of anisotropy were approximately 5% greater than the results when the anisotropy was included.

We can name various causes which affect the accuracy in the determination of  $B(E2)$ . One is the inaccuracy in determining the efficiency of the crystal for counting  $\gamma$  quanta under the full energy peak, others are the inaccuracy in determining  $dE/dpx$ , errors in the integrator, errors caused by the lack of definiteness in drawing the background curve under the peak, errors due to the energy spread of the  $\alpha$  particles in the beam, and finally errors due to counting statistics. According to our estimates, none of these errors exceed 10% and the overall error in determining  $B(E2)$  should be 25%. As a

check, we took the  $\gamma$ -ray spectra emitted after Coulomb excitation of Ta, Ag, Mo, and  $\text{Te}^{130}$ . The deviation of the average values of  $B(E2)$  for states excited in these nuclei in our experiments from data in the literature did not exceed 25%.

#### 4. RESULTS OF MEASUREMENTS AND DISCUSSION

##### 1. Even Isotopes of Tin

The data obtained for Coulomb excitation of even isotopes of tin are given in the table.  $\Delta E$  is the energy of the first excited state according to our data, while  $\Delta E^*$  is the energy obtained from studies of  $\beta$ -decay or inelastic scattering of neutrons.

The values of  $\Delta E$  found by us fill the gaps in the classification of energy values of first excited states of even-even isotopes of tin. Levels not previously known were found in  $\text{Sn}^{112}$ ,  $\text{Sn}^{118}$ , and  $\text{Sn}^{124}$ . For  $\text{Sn}^{120}$

and  $\text{Sn}^{116}$ , the data of various workers gave different values of  $\Delta E^*$ . In these cases, the data in the table enable us to make the correct choice. The observed trend in  $\Delta E$  with changing atomic number is possibly to be explained by the occurrence of a closed subshell at  $N = 64$ .

The excitation function was taken for each of the lines listed in the

Isotope	$\Delta E$ , Mev	$\Delta E^*$ , Mev	$\frac{B(E2)}{e^2} \cdot 10^{48}$ , $\text{cm}^4$	$\tau \cdot 10^{13}$ , sec	$F$	$B_1/B_2^*$	$C_2$ , Mev
$\text{Sn}^{112}$	1.26	—	0.18	7.2	11.1	16.3	280
$\text{Sn}^{114}$	1.30	1.3 [13]	0.20	5.5	12.0	14.2	266
$\text{Sn}^{116}$	1.29	1.27 [14] 1.3 [15]	0.19	6.0	11.2	14.9	285
$\text{Sn}^{118}$	1.22	—	0.19	8.0	11.0	15.7	276
$\text{Sn}^{120}$	1.18	1.18 [16] 1.3 [17]	0.17	10.5	9.6	18.0	304
$\text{Sn}^{122}$	1.15	1.14 [18]	0.15	13.5	8.2	20.8	344
$\text{Sn}^{124}$	1.13	—	0.14	15.9	7.6	22.6	370

table, and for the values of  $E_\alpha$  mentioned earlier. We observed no systematic change in  $B(E2)$  with changing  $E_\alpha$ . The values of  $B(E2)$  found for different values of  $E_\alpha$  remained constant within the limits of error of the experiment. This is evidence for the Coulomb character of the excitation. The table gives the average values of  $B(E2)/e^2$  found from a series of measurements including measurements for different values of  $E_\alpha$ . The average value of the rms error in determining  $B(E2)$  for the various isotopes was 20%. The largest rms error was 35% for  $\text{Sn}^{114}$ , and the smallest 15% for  $\text{Sn}^{124}$ . Levels with large values of  $\Delta E$  were excited in our work. The accuracy in estimating the efficiency of the crystal depends on  $E_\gamma$ . It is therefore especially interesting to compare values of  $B(E2)$  for excitation of states with large values of  $\Delta E$ . For this purpose we studied the Coulomb excitation of the state with  $\Delta E = 857$  kev ( $\Delta E = 850$  kev according to Ref. 1) in  $\text{Te}^{130}$ . According to our data the value of  $B(E2)/e^2$  is  $0.24 \times 10^{-48} \text{ cm}^4$ , while Ref. 1 gave  $0.26 \times 10^{-48} \text{ cm}^4$ .

From the table it follows that the values of  $B(E2)$  differ very little for all the even-even tin isotopes. The differences are within experimental error. The average value of  $B(E2)/e^2$  is approximately  $0.17 \times 10^{-48} \text{ cm}^4$ .

From the values of  $B(E2)$  and  $\Delta E$  determined in the experiment we can determine various other quantities characterizing the nucleus, in particular we can find the lifetime  $\tau$  of the first excited states of the even-even isotopes. Since the spin of these states is  $2^+$ , their de-excitation can occur only via an  $E2$  transition to the  $0^+$  ground state. The conversion coefficients for these transitions in tin are very small, so that in determining  $\tau$  we can use the formula given in Ref. 19 for the lifetime for a radiative transition with emission of a photon of multipolarity  $\lambda$  and energy  $\Delta E$ :

$$\frac{1}{\tau_\gamma(\lambda)} = \frac{8\pi(\lambda+1)}{\lambda[(2\lambda+1)!!]^2} \frac{1}{\hbar} \left( \frac{\Delta E}{\hbar c} \right)^{2\lambda+1} B(\lambda) \downarrow. \quad (13)$$

It follows that, for an  $E2$  transition ( $\lambda = 2$ ),

$$\frac{1}{\tau_\gamma(E2)} = \frac{4\pi}{75} \left( \frac{\Delta E}{\hbar c} \right)^5 \frac{1}{\hbar} B(E2) \downarrow, \quad (14)$$

where  $B(E2) \downarrow$  is the reduced probability of transition from the excited state to the ground state. According to the principle of detailed balancing, the values of  $B(E2) \downarrow$  and  $B(E2) \uparrow$  are related by

$$(2I_f + 1) B(E2) \downarrow = (2I_0 + 1) B(E2) \uparrow. \quad (15)$$

Since in our case  $I_0 = 0$ ,  $I_f = 2$ ,

$$B(E2) \downarrow = \frac{1}{5} B(E2) \uparrow. \quad (16)$$

Values of  $\tau$  calculated using formulas (14) and (16) are given in the table. The values of  $\tau$  determined in the experiment lie in the range from 5.5 to  $15.9 \times 10^{-13}$  sec. We note that satisfactory measurements of lifetimes using delayed coincidences have so far been limited to values of  $\tau$  greater than  $10^{-11}$  sec.

The quantity  $F$  given in the table is the ratio of  $B(E2) \uparrow$  to the quantity  $B(E2)_{s.p.} \uparrow$  calculated on the basis of the single-particle model:

$$B(E2)_{s.p.} \uparrow = 5 \left( \frac{1}{4\pi} \right) \left( \frac{3}{5} R_0^2 \right)^2.$$

In the computations we used  $R_0 \approx 1.2 A^{1/3} \times 10^{-13} \text{ cm}$ . It follows from the table that the value of  $F$  for even-even tin isotopes is approximately equal to 10. This is an indication of the collective nature of the excited states.

The last two columns of the table give the values of the parameters  $B_2/B_2^*$  and  $C_2$  which can be obtained from the experimental values of  $B(E2)$  and  $\Delta E$  if we assume that the first excited states of the even-even tin isotopes are vibrational levels. In the liquid drop model, for vibrations with small amplitude the expression for the energy can be expanded in a series in the amplitudes  $\alpha_{\lambda\mu}$  of oscillation of the electric multipole moment and their rates of change,  $\dot{\alpha}_{\lambda\mu}$ , so that in first approximation

$$H_{\text{vib}} = \sum \left\{ \frac{1}{2} B_\lambda (\dot{\alpha}_{\lambda\mu})^2 + \frac{1}{2} C_\lambda (\alpha_{\lambda\mu})^2 \right\}.$$

$B_\lambda$  is a parameter characterizing the mass transfer associated with the vibrations, and  $C_\lambda$  is the surface tension parameter. Since the surface deformation for  $\lambda = 1$  is simply a displacement of the mass, the lowest frequencies of collective oscillation correspond to quadrupole vibrations ( $\lambda = 2$ ). Reference 19

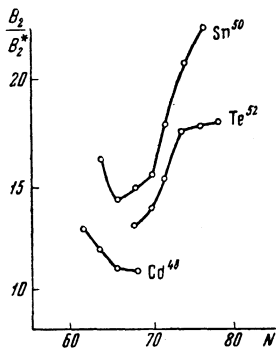


FIG. 6

FIG. 6. Dependence of  $B_2/B_2^*$  on neutron number  $N$  for even-even tin isotopes. For comparison with our data on tin, we give the data of Ref. 1 for Cd and Te.

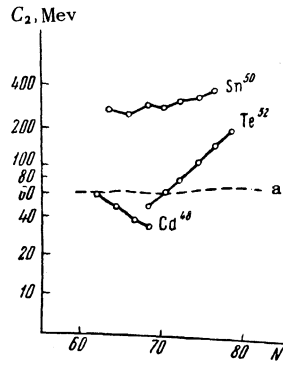


FIG. 7

FIG. 7. Dependence of  $C_2$  on neutron number for even-even tin isotopes. For comparison with our data on tin, we give data from Ref. 1 for Cd and Te; curve a shows the values of  $C_2$  according to the liquid drop model.

liquid drop model. It is interesting to note that, unlike cadmium and tellurium (which have almost the same  $Z$  as tin), the values of  $C_2$  for the tin isotopes change very little with changing neutron number.

The vibrational states have various characteristic features.<sup>19</sup> The energy of the second excited state is usually 2–2.5 times the energy of the first excited state. If the spin of the second level is  $2^+$ , the probability of an M1 transition to the first excited state with spin  $2^+$  is greatly reduced. In addition, the reduced probability for E2 transition from the second level to the ground state, which is forbidden for harmonic vibrations, is several orders of magnitude less than the transition probability to the first state. Finally, the cross section for Coulomb excitation of vibrational levels is approximately an order of magnitude greater than that for single-particle transitions, i.e.,  $F > 1$ . The fact that, according to our data,  $F \approx 10$ , does not exclude the possibility that the first excited levels of tin are single-particle levels, since collective interactions can increase the probability of a single-particle transition. To arrive at a definite conclusion concerning the nature of the first excited levels of the even-even tin isotopes, it would be important to excite the second levels. This problem is, however, much more complicated, both because of kinematic considerations as well as because the reduced transition probability from the ground state to the second state is much less than that to the first excited state.

## 2. Odd Isotopes of Tin

Our spectra of the Coulomb excitation of tin isotopes always contained two intense peaks, one peak at  $E = 75$  keV, due to the characteristic radiation from lead induced by the  $\alpha$  particles, and a peak with  $E = 511$  keV resulting from annihilation of positrons emitted from radioactive elements formed in  $(\alpha, n)$  reactions. We therefore investigated only the regions of the spectrum with energies from 0.1 to 0.4 MeV and energies above 0.75 MeV. No lines were found in the energy region from 0.1 to 0.4 MeV which could be attributed to Coulomb excitation. In the bombardment of  $\text{Sn}^{115}$ , we also found no lines in the region from 0.75 to 1.75 MeV. In bombardment of  $\text{Sn}^{119}$ , we found a line with  $E = 0.907$  MeV [ $B(E2)/e^2 = 0.11 \times 10^{-48} \text{ cm}^4$ ]. In bombarding  $\text{Sn}^{117}$ , we found two lines, with  $E = 0.865$  MeV [ $B(E2)/e^2 = 0.025 \times 10^{-48} \text{ cm}^4$ ] and  $E = 1.03$  MeV [ $B(E2)/e^2 = 0.09 \times 10^{-48} \text{ cm}^4$ ]. The values of  $B(E2)$  were calculated under the assumption that the values of the conversion coefficients for these transitions are small, and that the energies of the observed lines are equal to the excitation energies of the corresponding states. In other words, we assumed that these lines are not emitted as the result of a cascade from higher levels.

In the bombardment of  $\text{Sn}^{117}$ , we also found a composite peak, which we resolved into lines with  $E =$

gives formulas for determining  $B_2$  and  $C_2$  from experimental values of  $B(E2)$  and  $\Delta E$ :

$$B(E2) = 5 \left( \frac{3}{4\pi} ZeR_0^2 \right)^2 \frac{\hbar}{2(B_2 C_2)^{1/2}}; \quad \Delta E = \hbar \sqrt{C_2/B_2}.$$

The table gives the ratios  $B_2/B_2^*$ , where  $B_2^*$  is the value of the mass transfer parameter for the case of surface oscillations of an irrotational incompressible liquid drop.  $B_2^*$  is computed from the formula

$$B_2^* = \frac{3}{8\pi} AMR_0^2,$$

where  $A$  is the atomic number and  $M$  is the nucleon mass.

In Figs. 6 and 7, our values for  $B_2/B_2^*$  and  $C_2$  for the even-even isotopes of tin ( $Z = 50$ ) are compared with values of  $B_2/B_2^*$  and  $C_2$  for Cd ( $Z = 48$ ) and Te ( $Z = 52$ ) given in Ref. 1. The dashed curve in Fig. 7 shows the value of  $C_2$  obtained from the liquid drop model. According to the figures, the values of  $B_2/B_2^*$  are much greater than unity. The values of  $C_2$  are approximately 5 times as great as the value of  $C_2$  from the liquid drop model.



1.24 and 1.31 Mev. Study of the excitation function led us to the conclusion that these lines should be assigned to nuclear reactions which proceed via compound-nucleus formation.

- <sup>1</sup>G. M. Temmer and N. P. Heydenburg, Phys. Rev. **104**, 967 (1956).
- <sup>2</sup>Fagg, Geer, and Wolicki, Phys. Rev. **104**, 1073 (1956).
- <sup>3</sup>K. Alder and A. Winther, CERN report, October 1955.
- <sup>4</sup>Alkhazov, Andreev, Grinberg, and Lemberg, Izv. Akad. Nauk SSSR, Ser. Fiz. **20**, 1365 (1956), [translated by Columbia Technical Translations **20**, 1249 (1956)].
- <sup>5</sup>Alkhazov, Andreev, Grinberg, and Lemberg, Nucl. Phys. **2**, 65 (1956).
- <sup>6</sup>Fagg, Wolicki, Bondelid, Dunning, and Snyder, Phys. Rev. **100**, 1299 (1955).
- <sup>7</sup>V. P. Rybakov, J. Exptl. Theoret. Phys. (U.S.S.R.) **28**, 651 (1955), Soviet Phys. JETP **1**, 435 (1955).
- <sup>8</sup>E. Segre, *Experimental Nuclear Physics*, Wiley, New York, 1953.
- <sup>9</sup>Maeder, Muller, and Wintersteiger, Helv. Phys. Acta **27**, 465 (1954).
- <sup>10</sup>C. M. Davisson and R. D. Evans, Revs. Mod. Phys. **24**, 79 (1952).
- <sup>11</sup>S. A. Baranov and R. M. Polevoi, "Counter for Absolute Counting of Charged Particles," All-Union Conference on Application of Radioactive and Stable Isotopes, Moscow, 1957.
- <sup>12</sup>Rietjens, Arkenbout, Wolters, and Kluyver, Physica **21**, 110 (1955).
- <sup>13</sup>L. Grodzins and H. Motz, Bull. Amer. Phys. Soc. **30**, #7, 9 (1955).
- <sup>14</sup>Slätis, du Toit, and Siegbahn, Ark. f. Fys. **2**, 321 (1951).
- <sup>15</sup>Aten, Manassen, and Feyfer, Physica **20**, 665 (1954).
- <sup>16</sup>C. L. McGinnis, Phys. Rev. **98**, 1172(A) (1955).
- <sup>17</sup>Blaser, Boehm, and Marmier, Helv. Phys. Acta **23**, 623 (1950).
- <sup>18</sup>Farrelly, Koerts, van Lieshout, Benczer, and Wu, Phys. Rev. **98**, 1172(A) (1955).
- <sup>19</sup>Alder, Bohr, Huus, Mottelson, and Winther, Revs. Mod. Phys. **28**, 432 (1956).

Translated by M. Hamermesh

278

SOVIET PHYSICS JETP

VOLUME 6 (33), NUMBER 6

JUNE, 1958

# ON THE THERMODYNAMICAL THEORY OF RELAXATION PHENOMENA IN SYSTEMS WITH ADDITIONAL PARAMETERS

V. T. SHMATOV

Ural' Branch, Academy of Sciences, U.S.S.R.

Submitted to JETP editor April 17, 1957; resubmitted June 26, 1957

J. Exptl. Theoret. Phys. (U.S.S.R.) **33**, 1359-1362 (1957)

A thermodynamical theory of relaxation phenomena connected with the relaxation of an additional internal parameter of the system is developed on the basis of the method of Mandel'shtam and Leontovich. The relaxation times and the relation between them are established. Expressions are obtained for the dynamic derivatives of a system undergoing a periodic perturbation. A relation is found between the relaxation times and discontinuities in the derivatives near the Curie point. The results are extended to an arbitrary number of additional internal parameters.

THE term "additional internal parameter" is applied to a quantity characterizing some internal property of a system which, when the system is in equilibrium, appears to be a function of state. A delay on the part of the additional parameters in responding to external influences on the system leads, for example, to re-